
Overcoming Catastrophic Forgetting in Federated Class-Incremental Learning via Federated Global Twin Generator

Thinh Nguyen¹, Khoa D Doan¹, Binh T. Nguyen², Danh Le-Phuoc³, Kok-Seng Wong¹

¹College of Engineering & Computer Science, VinUniversity, Hanoi, Vietnam

²Vietnam National University - Ho Chi Minh city, University of Science, Vietnam

³Technische Universität Berlin, Germany

{thinh.nth, khoa.dd, wong.ks}@vinuni.edu.vn

ngtbinh@hcmus.edu.vn, danh.lephuoc@tu-berlin.de

Abstract

Federated Class-Incremental Learning (FCIL) increasingly becomes important in the decentralized setting, where it enables multiple participants to collaboratively train a global model to perform well on a sequence of tasks without sharing their private data. In FCIL, conventional Federated Learning algorithms such as FedAVG often suffer from catastrophic forgetting, resulting in significant performance declines on earlier tasks. Recent works, based on generative models, produce synthetic images to help mitigate this issue across all classes, but these approaches' testing accuracy on previous classes is still much lower than recent classes, i.e., having better plasticity than stability. To overcome these issues, this paper presents Federated Global Twin Generator (FedGTG), an FCIL framework that exploits privacy-preserving generative-model training on the global side without accessing client data. Specifically, the server trains a data generator and a feature generator to create two types of information from all seen classes, and then it sends the synthetic data to the client side. The clients then use feature-direction-controlling losses to make the local models retain knowledge and learn new tasks well. We extensively analyze the robustness of FedGTG on natural images, as well as its ability to converge to flat local minima and achieve better-predicting confidence (calibration). Experimental results on CIFAR-10, CIFAR-100, and tiny-ImageNet demonstrate the improvements in accuracy and forgetting measures of FedGTG compared to previous frameworks.

1 Introduction

Federated Learning (FL) [1, 2] is a Machine Learning setting that facilitates collaborative learning while maintaining privacy. Despite its significant achievements on various domains [3–6], FL observes several critical challenges, including resource limitation and data heterogeneity. Moreover, the client's local data distribution is assumed to remain unchanged, but the real-world scenarios [7] can be totally different, where the client's task, data, and domain can be changed, as shown in Figure 1. To overcome such challenges, Federated Class-Incremental Learning (FCIL) [8, 9] is an innovative approach that combines the principles of FL and Class-Incremental Learning (CIL) [10] to enable models to learn continuously from decentralized data sources while adapting to new information over time without forgetting previous knowledge [11]. This approach addresses data privacy challenges and ensures the model can evolve as new data types or tasks emerge without needing to access historical data. In CIL, exemplar-based approaches [10, 12, 13] preserve a limited number of samples

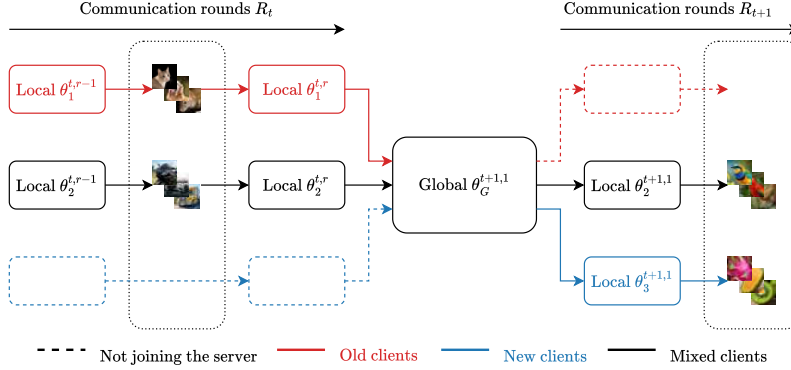


Figure 1: Illustration of the real-world scenarios in the FCIL setting.

from previous tasks to prevent forgetting, whereas exemplar-free approaches [14–16] do not retain any samples from prior tasks.

Due to privacy concerns in many FL systems (e.g., hospitals and research areas), users cannot store any historical data, so the exemplar-free category is of particular interest. Recent works [17–19] in this field tend to generate synthetic data and combine with distilling regularizers [20, 15] to balance the trade-off between retaining knowledge and learning new tasks. However, experimental results have shown that these works still witness catastrophic forgetting, i.e., bias towards recent classes; see Figure 2a and 2b.

To address this problem, we propose **Federated Global Twin Generator (FedGTG)**, an FCIL framework that does not store any data from clients. After completing one task, the server trains two generative models and shares them with clients on subsequent tasks to create synthetic examples and features of previous classes. On the client side, we propose a synthetic logit distillation using generated features for retaining knowledge, as well as a fine-tuning loss using both real and generated data to balance the ability to predict all classes. However, using only these two objectives still hinders the model’s ability to obtain new knowledge, see Figure 2c. We argue that this issue happened as the feature directions were not constrained. Therefore, we add a feature-direction-controlling loss, which helps the model to have more plasticity in learning new tasks. As a result, FedGTG achieved extensive performance in terms of accuracy and forgetting measures compared to previous methods, as shown in Section 4.2.

We summarize our contributions below:

- We propose an FCIL framework ensuring clients’ privacy by training a data generator and a feature generator on the server side. These generators are distributed to the clients to mitigate catastrophic forgetting.
- On the client side, we propose direction-controlling objectives to help the model have a better stability-plasticity trade-off.
- We demonstrate the effectiveness of our method in popular benchmarks, including CIFAR-10, CIFAR-100, and tiny-ImageNet, with a 4% increase in accuracy and a 10% decrease in forgetting.
- We analyze the robustness of FedGTG compared with recent FCIL algorithms on natural images, as well as test its abilities to converge to flat minima and achieve better predicting confidence.

2 Related work and preliminaries

2.1 Continual Learning

Catastrophic forgetting [11] is a major issue in machine learning where training a model on new data makes it forget its previously learned knowledge. This issue is central to the field of CL, whose primary objective is to build models to acquire new knowledge while retaining information from older tasks. Numerous strategies have been explored to mitigate this problem, including the implementation of regularization terms [21–23], the isolation of architectural parameters [24–26], the use of experience

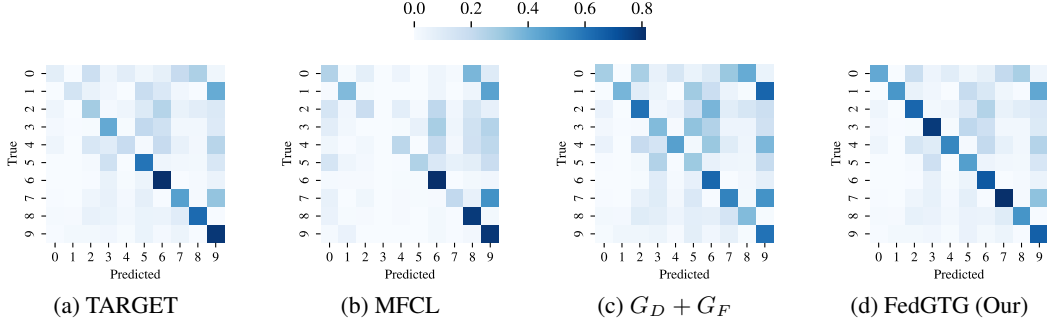


Figure 2: Confusion matrix among FCIL algorithms: **(a)** TARGET, **(b)** MFCL, **(c)** only the application of two generators to FL, and **(d)** FedGTG, testing on CIFAR-10 after training is completed. While TARGET and MFCL have bad predicting performance on initial classes and two generators struggle to learn new tasks, FedGTG achieves a better stability-plasticity trade-off.

replay through data storage [10, 12, 13], and studies of data generation [14–16]. In CL, replay-based methods observe significant performance in terms of accuracy and forgetting measures. However, due to privacy concerns in FCIL, privacy concerns prevent data storage, making these methods inapplicable. An extensive alternative to address this issue is generative-based approaches.

Learning tasks There are three main types of learning in CL: Task-Incremental Learning (Task-IL), Domain-Incremental Learning (Domain-IL), and Class-Incremental Learning (Class-IL) [27]. In Task-IL, each task is distinct and comes with its own distribution during training and testing. In Domain-IL, the learning task does not change, while different domains or distributions of data sequentially arrive during training. In Class-IL, each new task adds new classes to what the model has to learn, which continually expands the amount of information the model needs to handle.

2.2 Federated Class-Incremental Learning

The goal of FCIL is to train a model to learn new classes over time without forgetting previously learned classes while also ensuring that data privacy is maintained across multiple decentralized devices. Several approaches exploit Knowledge Distillation [20] to mitigate forgetting by appointing the global model’s weight of the most recent task as a teacher. **Continual Federated Learning with Distillation (CFed)** [28] constructs server and client-side knowledge distillation using a surrogate dataset, but this costs time and financial resources to collect enough data for this surrogate dataset. **Global-Local Forgetting Compensation (GLFC)** [8] relaxes this problem by training a proxy server globally to ease the imbalance issue between classes.

The above approaches yield extensive performance in past knowledge retention but lack the ability to learn well on new tasks. To alleviate this issue, **Federated Class-Incremental Learning (FedCIL)** [18] trains generators at both client-side and server-side, as well as utilizing knowledge distillation to balance the stability-plasticity trade-off. However, this approach can raise a privacy risk since information about client-side generative models is shared with the server. **Federated Class-Continual Learning via Exemplar-Free Distillation (TARGET)** [17] and **Mimicking Federated Continual Learning (MFCL)** [19] ensures clients’ privacy and limited storage by training a data generator on the global-side and adding distilling regularizers to the client-side training to enhance overall performance. However, as we show in Figure 2, these methods still have bad performance on old classes, leaving catastrophic forgetting mitigation a still desirable goal.

2.3 Preliminaries

There are c clients, denoted as $\{C_1, C_2, \dots, C_c\}$ and a central server, denoted as S . We consider the Synchronous Federated Continual Learning setting [29] where all clients share the same task sequence $T = \{T_1, T_2, \dots, T_n\}$. Specifically, at task T_i , each client C_i has a private dataset $\mathcal{D}_i^t = \{\mathcal{X}_i^t, \mathcal{Y}^t\}$.

During the first task, the global model θ_G^1 is obtained after aggregating local models $\{\theta_1^1, \theta_2^1, \dots, \theta_{s_1}^1\}$ using conventional Deep Learning methods, where s_1 is a number of selected clients among all. From

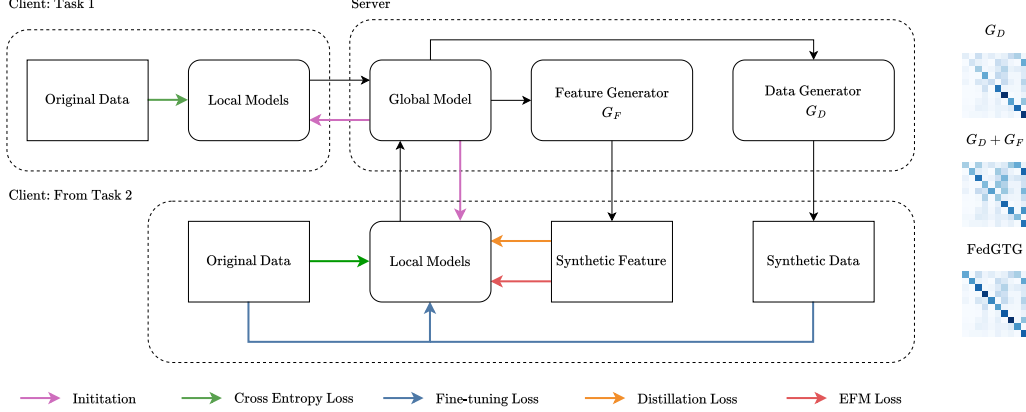


Figure 3: Illustration of the proposed framework. After completing one task, the server employs a data-free approach to train two generators. The clients then use two types of synthetic information from these generators to train their local models for retaining knowledge and learning new tasks well.

the task T_t , $t \geq 2$, the global model θ_G^{t-1} can distinguish the samples belonged to the classes set $\bigcup_{i=1}^{t-1} \mathcal{Y}_i$. The server then distributes its parameters back to the clients. Client C_i uses θ_G^{t-1} as an initial model to train on task T_t using its private dataset \mathcal{D}_i^t . The local model θ_i^t should perform well in classifying classes from the set $\bigcup_{i=1}^t \mathcal{Y}_i$. Finally, the server collects the local models from clients who participate in the process after each r_t communication round and obtains a new global model θ_G^t , which can identify classes from the set $\bigcup_{i=1}^t \mathcal{Y}_i$.

3 Methodology

3.1 Overview

Several approaches [10, 12, 13] in the conventional CL achieve significant predicting performance across all classes by storing a small subset of samples from previous tasks in episodic memory. However, this approach is not viable in the FL setting due to privacy concerns (e.g., local hospitals cannot share data with the central server). One initial approach to address this challenge is using generative models, which can generate synthetic data for subsequent training, as demonstrated in earlier studies [17, 19]. However, as illustrated in Figure 2, only generating synthetic examples still causes catastrophic forgetting in previously learned classes. Therefore, we propose a Federated Global Twin Generator (FedGTG), which can balance the stability-plasticity trade-off and clients' privacy. This method has two main stages: (1) At the end of each task, the server trains a data generator and a feature generator to capture the information of all seen classes; (2) Clients receive generators from the server to create synthetic information, as well as obtaining global weights as initialization, which helps retain knowledge from previous tasks and learn the new task efficiently. In the following section, we will explain these two stages of FedGTG (Figure 3).

3.2 Server-side

3.2.1 Data Generator

Since the server only has access to the global model's weights, we can only train the data generator using data-free methods, such as DeepInversion. Specifically, we have a generative model that takes a noise $z \sim \mathcal{N}(0, 1)$ as input and produces a synthetic example \tilde{x} mirroring the dimensions of the original training input. This synthetic data should observe the following objectives.

After training task T_t , the synthetic data should be classified correctly by the global model θ_G^t , and they should not be biased to any classes. With this aim, we employ a temperature cross entropy classification loss between its assigned label z and the prediction of θ_G^t on $G_D^t(z)$ as

$$\mathcal{L}_{\text{CE}} = \text{CE}_{\text{last}}(\text{argmax}(z[:, q]), \theta_G^t(\tilde{x})) + \lambda_{\text{current}} \text{CE}_{\text{current}}(\text{argmax}(z[:, q]), \theta_G^t(\tilde{x})), \quad (1)$$

where \tilde{x} is the output of $G_D^t(z)$, CE_{last} and $\text{CE}_{\text{current}}$ respectively are the Cross-Entropy Loss using the truncated outputs of $\theta_G^t(\tilde{x})$ corresponding with last classes from task T_i , $i < t$, and current learned classes on task T_t , and λ_{current} is the temperature hyper-parameter.

Generating synthetic examples can easily be biased to a subset of classes. To maintain the diversity between classes, we utilize the Information Entropy (IE) Loss [30] as follows:

$$\mathcal{L}_{\text{IE}} = -\mathbf{H}_{\text{info}} \left(\frac{1}{\text{bs}} \sum_{i=1}^{\text{bs}} \theta_G^t(\tilde{x}_i) \right), \text{ bs: batch size,} \quad (2)$$

This loss measures the IE for samples of a batch. By maximizing this value, we can promote a more uniform and balanced output distribution from the generator across all classes.

In order to further improve the stability of generator training, we use Batch Normalization Loss [31] to make all Batch Normalization layers have the same statistics on synthetic images, as follows:

$$\mathcal{L}_{\text{batch}} = \frac{1}{L} \sum_{j=1}^L \text{KL}(\mathcal{N}(\mu_j, \sigma_j^2) \parallel \mathcal{N}(\tilde{\mu}_j, \tilde{\sigma}_j^2)), \quad (3)$$

where L is the total number of Batch Normalization layers in the architecture of the global model. μ_j and σ_j^2 are the mean and variance stored in Batch Normalization layer j of the global model, $\tilde{\mu}_j$ and $\tilde{\sigma}_j^2$ are measured statistics of Batch Normalization layer j for the synthetic data.

Adjacent pixels in real images typically have values that are near to one another. One typical method to promote similar patterns in the synthetic images is to add Image Prior Loss [32]. We can create the smoothed (blurred) version of an image by applying a Gaussian kernel and minimizing the distance of the original and Smooth(\tilde{x}) as

$$\mathcal{L}_{\text{smooth}} = \|\tilde{x} - \text{Smooth}(\tilde{x})\|_2^2. \quad (4)$$

In summary, we can write the training objective of G_D as follows:

$$\min_{G_D} \mathcal{L}_{\text{CE}} + \lambda_{\text{IE}} \mathcal{L}_{\text{IE}} + \lambda_{\text{batch}} \mathcal{L}_{\text{batch}} + \lambda_{\text{smooth}} \mathcal{L}_{\text{smooth}}, \quad (5)$$

where λ_{IE} , λ_{batch} , and λ_{smooth} are hyper-parameters of specific loss functions.

3.2.2 Feature Generator

As mentioned in Section 3.1, only synthetic images can exacerbate the catastrophic forgetting problem. To address this, we train a feature generator that synthesizes features, capturing the knowledge within the feature space. Like the data generator, this generative model is trained only on the server side. The feature generator takes noise input $z \sim \mathcal{N}(0, 1)$ and produces synthetic features \tilde{f} that match the dimensions of the original features. These synthetic features must meet the following objectives:

Temperated Cross Entropy Loss After training task T_t , the generative feature should be classified correctly by the classifier H_G^t of the global model. Additionally, the synthetic features should not be biased to any classes. With this aim, we employ a temperature cross entropy classification loss between its assigned label z and the prediction of H_G^t on $G_D^t(z)$ as

$$\mathcal{L}_{\text{FCE}} = \text{CE}_{\text{last}} \left(\text{argmax}(z[:, q]), H_G^t(\tilde{f}) \right) + \lambda_{\text{current}} \text{CE}_{\text{current}} \left(\text{argmax}(z[:, q]), H_G^t(\tilde{f}) \right), \quad (6)$$

where \tilde{f} is the output of $G_F^t(z)$, CE_{last} and $\text{CE}_{\text{current}}$ respectively are the Cross Entropy Loss using the truncated outputs of $H_G^t(\tilde{f})$ corresponding with last classes from task T_i , $i < t$, and current learned classes on task T_t , and λ_{current} is the temperature hyper-parameter.

Feature Information Entropy Loss The generated features should also not be biased to any subset of classes. Therefore, we adjust the IE Loss (Equation 2) and propose the Feature Information Entropy Loss to make the synthetic feature have this quality, which is

$$\mathcal{L}_{\text{FIE}} = -\mathbf{H}_{\text{info}} \left(\frac{1}{\text{bs}} \sum_{i=1}^{\text{bs}} H_G^t(\tilde{f}_i) \right), \text{ bs: batch size,} \quad (7)$$

In summary, we can write the training objective of G_F as follows:

$$\min_{G_F} \mathcal{L}_{\text{FCE}} + \lambda_{\text{FIE}} \mathcal{L}_{\text{FIE}}, \quad (8)$$

where λ_{FIE} is the hyper-parameter of Feature Information Entropy Loss.

3.3 Client-side

From task $T_{t \geq 2}$, on the client side, we have to solve the trade-off between learning the current task quickly (plasticity) and retaining knowledge from previous tasks efficiently (stability). To this end, we divide the learning objectives into two parts.

Plasticity To learn new tasks well, the model needs to learn the new information in a way that is separate from the old classes. To do this, we compute the Cross-Entropy Loss by using only the new classes' linear heads. Formally, we minimize:

$$\mathcal{L}_{\text{CE}} = \text{CE}(\theta^t(x | T_t), y), \quad (9)$$

where $\theta^t(x | T_t)$ is model's output and masking old classes before task T_t 's linear heads.

Stability To mitigate forgetting, previous approaches leverage knowledge distillation [33, 17]. However, this can cause information loss in probability space due to squashing functions [34]. Therefore, motivated by Buzzega et al. [13], we propose Synthetic Logits Distillation Loss, which matches the logits of the old and current linear heads. These classifiers take synthetic features as input instead of synthetic data since the feature stores more previous information. Formally, we optimize:

$$\mathcal{L}_{\text{logits}} = \left\| \theta_G^{t-1}(\tilde{f}) - \theta^t(\tilde{f}) \right\|, \quad (10)$$

where θ_G^{t-1} is the global model trained up to task T_{t-1} .

As shown in [13], when there is a sudden shift in the distribution of the input of the task sequence, biased features on previous tasks can output biased logits, hindering the ability to obtain new knowledge. To mitigate this shortcoming, from task T_t , we leverage synthetic data by training it alongside with real data. However, the distribution of synthetic data may vary from that of real data, making it essential to ensure the model does not distinguish between old and new data solely based on these differences. To address this problem, we only use the extracted features of the data. To tackle this issue, we utilize only the extracted features of the data, i.e., clients freeze the feature extraction layers and update only the linear head (represented by H^t) for both real (x) and synthetic (\tilde{x}) images. This Fine-tuning loss is formulated as

$$\mathcal{L}_{\text{FT}} = \text{CE}\left(H^t\left(\begin{bmatrix} f \\ \tilde{f} \end{bmatrix}\right), [y, \tilde{y}]\right), \quad (11)$$

where f and \tilde{f} respectively are the extracted features of x and \tilde{x} after passing through the frozen feature extractor F^t of the local model, y and \tilde{y} is the hard label of x and \tilde{x} .

Enhancing stability-plasticity Figure 2c shows that the combination of the above objectives reduces the model's performance across all classes. We contend that this happens because the feature directions are unconstrained, resulting in the total loss failing to converge. We then further add additional loss to balance this problem, named Empirical Feature Matrix Loss [16], which constrains directions in feature space most important for previous tasks, while it allows more plasticity in other directions when learning new tasks. In this work, we re-utilize the synthetic features to calculate the Empirical Feature Matrix E_{t-1} from the previous task T_{t-1} . We have,

$$\mathcal{L}_{\text{EFM}} = (F^t(x) - F_G^{t-1}(x))^\top (\lambda_E E_{t-1} + \eta I) (F^t(x) - F_G^{t-1}(x)), \quad (12)$$

where F^t and F_G^{t-1} respectively are the feature extractor of the current model and the previous global model, η is the damping term to constrain features to stay in a specific region.

In summary, the final objective on the client side as

$$\min_{\theta^t} \mathcal{L}_{\text{CE}} + \lambda_{\text{logits}} \mathcal{L}_{\text{logits}} + \lambda_{\text{FT}} \mathcal{L}_{\text{FT}} + \lambda_{\text{EFM}} \mathcal{L}_{\text{EFM}}. \quad (13)$$

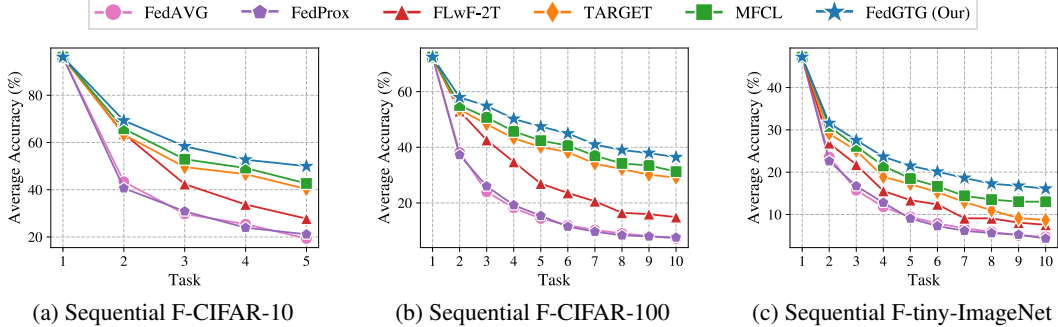


Figure 4: Average Accuracy per task of various algorithms on popular benchmarks.

Table 1: Performance of the different baselines in terms of AIA and AF for three datasets. [↑] higher is better, [↓] lower is better.

Method	CIFAR-10		CIFAR-100		tiny-ImageNet	
	AIA [↑]	AF [↓]	AIA [↑]	AF [↓]	AIA [↑]	AF [↓]
FedAVG	42.82 ± 0.23	55.55 ± 0.58	21.39 ± 0.22	78.67 ± 0.83	13.80 ± 0.19	74.12 ± 0.81
FedProx	42.43 ± 0.32	56.15 ± 0.71	21.54 ± 0.32	78.12 ± 0.71	13.69 ± 0.21	75.16 ± 0.79
FLwF-2T	52.74 ± 0.23	39.51 ± 0.59	32.19 ± 0.18	50.78 ± 0.63	17.18 ± 0.17	44.51 ± 0.67
TARGET	59.19 ± 0.16	17.23 ± 0.45	42.15 ± 0.13	26.45 ± 0.61	19.46 ± 0.25	20.17 ± 0.57
MFCL	61.34 ± 0.21	22.32 ± 0.52	45.07 ± 0.12	28.30 ± 0.78	21.47 ± 0.15	23.90 ± 0.58
FedGTG (Our)	64.50 ± 0.22	13.14 ± 0.67	46.42 ± 0.18	18.66 ± 0.76	24.04 ± 0.23	16.18 ± 0.62

4 Experimental results

4.1 Experimental Setup

In this section, we provide our experimental setup, including the datasets used, FCIL baselines, and implementation details.

Datasets We perform our experiments on three widely-used benchmark datasets in FCIL [8, 17, 19], which are the protocol versions in the FCIL setting of **CIFAR-10** [35], **CIFAR-100** [35], **tiny-ImageNet** [36], and we name it respectively are **Sequential F-CIFAR-10**, **Sequential F-CIFAR-100** and **Sequential F-tiny-ImageNet**. The data preparation is explained later in Appendix B. We use Latent Dirichlet Allocation (LDA) [37] with $\alpha = 1$ to distribute the data of each task among clients.

FCIL Baselines In addition to our FedGTG, we also include one regularization-based method, **FLwF-2T** [33], and two generative-based methods, **TARGET** [17] and **MFCL** [19]. The detailed description of these algorithms can be seen in Appendix B.

Models and Implementation Details In all experiments, we train a ResNet-18 [38] backbone using the SGD optimizer [39]. We train the model for 100 epochs per task on every dataset. Additional implementation details and hyper-parameter configurations are then provided in the Appendix B.

Evaluation Metrics We report the performance of the methods using two metrics: Average Incremental Accuracy and Average Forgetting. **Average Incremental Accuracy (AIA)** measures the average accuracy of the global model on all tasks after the training finishes. Forgetting (f_t) of task T_t is the difference between the model’s best performance on task T_t and its accuracy after completed training. Consequently, **Average Forgetting (AF)** is the average of all f^t , from task T_1 to task T_{n-1} , at the end of task T_n . We report the averaged result over three different random initializations.

4.2 Performance Results

We present the performance of FedGTG and the baselines. Figure 4 shows the Average Accuracy of the model at each task in the training process. It can be seen that FedGTG achieves state-of-the-art

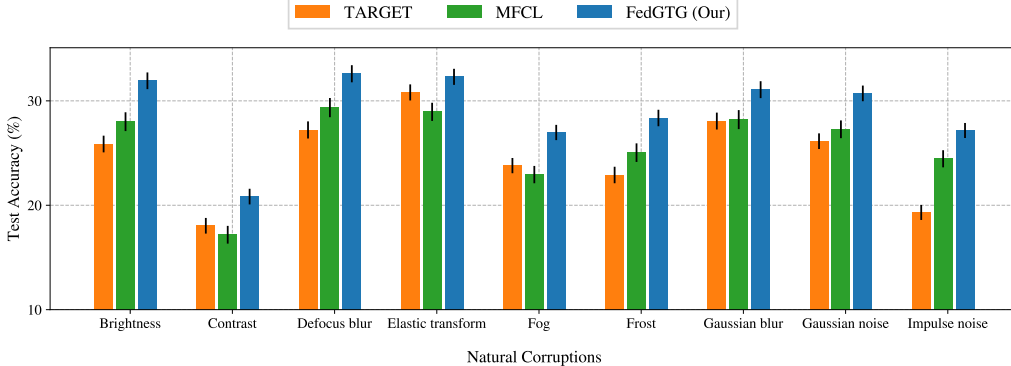


Figure 5: Robustness to natural corruptions.

performance in all settings. Specifically, our method observes better Average Accuracy on all later tasks. Table 1 reports both AIA results (*higher is better*) and AF results (*lower is better*).

As expected, FedAvg and FedProx suffer the highest forgetting since they are not designed for FCIL. When compared to FLwF-2T, the performance gap between it and our FedGTG is significant, indicating that regularization towards previous parameter sets is insufficient to avoid forgetting. Compared to the generative-replay methods, TARGET and MFCL, our FedGTG achieves the least AF and the best AIA, showing that FedGTG can both retain knowledge and learn new tasks effectively.

4.3 Model Analysis

The majority of FCIL research concentrates on testing experiments on ideal benchmarks [8, 17, 19], such as CIFAR [35] and ImageNet [40]. This results in a lack of analysis concerning real-world scenarios, such as the decision-making ability required in hospitals or the model’s generalization to diverse environments. Therefore, in this section, we conducted experiments to analyze the robustness of FedGTG and three FCIL algorithms mentioned above on corrupted environments, as well as the qualities of generalization [41–43] and achieve calibrated networks [44, 45].

Robustness to natural corruptions In the real world, autonomous cars must operate effectively in various environments, including diverse weather conditions. Therefore, it is essential for FCIL algorithms to be robust to naturally corrupted data distributions. We then evaluate our method and the recent FCIL methods on the **CIFAR-100-C** dataset. This dataset includes 18 augmentations of the original CIFAR-100, inspired by CIFAR-10-C [46]. Models are trained using standard CIFAR-100 with the same setting in Section 4.1 and tested on CIFAR-100-C. Figure 5 shows robustness to 09 different corruptions averaged over three different runs, the results of the rest augmentations are shown in the Appendix D. Specifically, our approach achieves higher test accuracy on various corruptions, with an average improvement of 5% over MFCL and 8% over TARGET. Evidently, our method offers noticeable advantages in robustness against natural corruption.

Converging to flatter minima Extensive CL algorithms [47–49] explore how well their methods generalize by examining their ability to converge to flat minima. If a model obtains this quality, the loss function values \mathcal{L}_{CE} increase only slightly, suggesting stable model predictions and demonstrating good train-test generalization. In this part, we compare the flatness of the training minima of FLwF-2T, TARGET, and MFCL with our approach. As done in [50], we consider the model at the end of training and add independent Gaussian noise with growing variance to each parameter. This allows us to evaluate its effect on the average loss $\sum_{t=1}^n \mathcal{L}_{CE}^{(T_t)}$ across all training examples. As shown in Figures 6a and 6b, MFCL, especially FLwF-2T and TARGET, reveal higher sensitivity to perturbations than FedGTG. This result concludes that FedGTG can achieve better generalization compared to previous methods.

Converging to a more calibrated network Calibration measures how well a learner’s prediction confidence matches its accuracy, with ideal outcomes reflecting true probabilities of correctness. In real-world applications, including weather forecasting [51] and econometric analysis [52], the

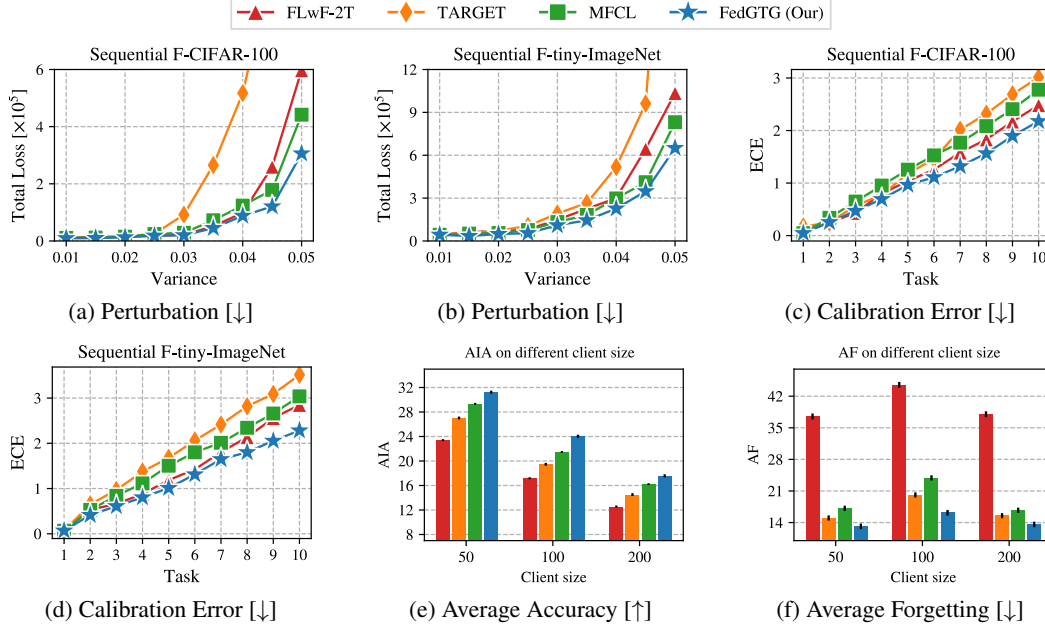


Figure 6: Results for the model analysis. [\uparrow] higher is better, [\downarrow] lower is better (*best seen in color*).

calibrating ability of an FCIL algorithm should be investigated. Figures 6c and 6d show the value of the Expected Calibration Error (ECE) [53] across various FCIL methods after completing each task. It can be seen that FedGTG achieves a lower ECE than the others. This indicates that models trained with FedGTG are less over-confident and, consequently, easier to interpret.

Robustness to different client sizes We validate the effectiveness of FedGTG compared to other FCIL algorithms across different client sizes on the tiny-ImageNet dataset. We run experiments by varying the number of total clients (maintaining a consistent participation rate of 0.1 per round), ranging from 50 to 200, and compare the results. Figures 6e and 6f demonstrate that our method still outperforms other approaches, achieving an accuracy 4% higher and a forgetting rate 6% lower compared to the next best method, MFCL.

4.4 Limitations

In our work, clients require generative models, the global model’s weight from the most previous task, and the current global model, which raises storage burdens between the server and clients. However, there are more benefits than storing actual data. First, the memory required for the generative models does not depend on the class size: as the number of classes increases, clients may need to either delete some stored examples to make space for new ones or expand their memory capacity. In contrast, the size of the generative models remains constant. Moreover, clients can remove the generative models when inactive during a specific round and retrieve them later when rejoining, whereas removing data samples leads to a permanent loss of information.

5 Conclusion

This study introduces an FCIL framework that tackles the constraints of limited resources and privacy concerns. We utilize data and feature generative models that have been trained by the server, eliminating the requirement for costly on-device memory for clients. Our experiments provide evidence that our strategy is successful in reducing catastrophic forgetting and surpasses the current state-of-the-art methods. This paper also analyzes the robustness of FCIL algorithms on natural images, as well as testing the qualities of converging to flat minima and calibrated networks.

References

- [1] H Brendan McMahan, Eider Moore, Daniel Ramage, and Blaise Agüera y Arcas. Federated learning of deep networks using model averaging. *arXiv preprint arXiv:1602.05629*, 2:2, 2016.
- [2] Keith Bonawitz, Hubert Eichner, Wolfgang Grieskamp, Dzmitry Huba, Alex Ingerman, Vladimir Ivanov, Chloe Kiddon, Jakub Konečný, Stefano Mazzocchi, Brendan McMahan, et al. Towards federated learning at scale: System design. *Proceedings of machine learning and systems*, 1:374–388, 2019.
- [3] Keval Doshi and Yasin Yilmaz. Federated learning-based driver activity recognition for edge devices. In *Proceedings of the IEEE/CVF Conference on Computer Vision and Pattern Recognition*, pages 3338–3346, 2022.
- [4] Bill Yuchen Lin, Chaoyang He, Zihang Zeng, Hulin Wang, Yufen Huang, Mahdi Soltanolkotabi, Xiang Ren, and Salman Avestimehr. Fednlp: A research platform for federated learning in natural language processing. *arXiv preprint arXiv:2104.08815*, 2021.
- [5] Yunyi Liu and Ruining Yang. Federated learning application on depression treatment robots (dtbot). In *2021 IEEE 13th International Conference on Computer Research and Development (ICCRD)*, pages 121–124. IEEE, 2021.
- [6] Thien Duc Nguyen, Samuel Marchal, Markus Miettinen, Hossein Fereidooni, N Asokan, and Ahmad-Reza Sadeghi. Ddot: A federated self-learning anomaly detection system for iot. In *2019 IEEE 39th International conference on distributed computing systems (ICDCS)*, pages 756–767. IEEE, 2019.
- [7] Rahaf Aljundi. Continual learning in neural networks. *arXiv preprint arXiv:1910.02718*, 2019.
- [8] Jiahua Dong, Lixu Wang, Zhen Fang, Gan Sun, Shichao Xu, Xiao Wang, and Qi Zhu. Federated class-incremental learning. In *Proceedings of the IEEE/CVF conference on computer vision and pattern recognition*, pages 10164–10173, 2022.
- [9] Jiahua Dong, Hongliu Li, Yang Cong, Gan Sun, Yulun Zhang, and Luc Van Gool. No one left behind: Real-world federated class-incremental learning. *IEEE Transactions on Pattern Analysis and Machine Intelligence*, 2023.
- [10] Sylvestre-Alvise Rebuffi, Alexander Kolesnikov, Georg Sperl, and Christoph H Lampert. icarl: Incremental classifier and representation learning. In *Proceedings of the IEEE conference on Computer Vision and Pattern Recognition*, pages 2001–2010, 2017.
- [11] Robert M French. Catastrophic forgetting in connectionist networks. *Trends in cognitive sciences*, 3(4): 128–135, 1999.
- [12] Arslan Chaudhry, Marcus Rohrbach, Mohamed Elhoseiny, Thalaiyasingam Ajanthan, Puneet K Dokania, Philip HS Torr, and Marc’Aurelio Ranzato. On tiny episodic memories in continual learning. *arXiv preprint arXiv:1902.10486*, 2019.
- [13] Pietro Buzzega, Matteo Boschini, Angelo Porrello, Davide Abati, and Simone Calderara. Dark experience for general continual learning: a strong, simple baseline. *Advances in neural information processing systems*, 33:15920–15930, 2020.
- [14] Chen He, Ruiping Wang, Shiguang Shan, and Xilin Chen. Exemplar-supported generative reproduction for class incremental learning. In *BMVC*, volume 1, page 2, 2018.
- [15] Xialei Liu, Chenshen Wu, Mikel Menta, Luis Herranz, Bogdan Raducanu, Andrew D Bagdanov, Shangling Jui, and Joost van de Weijer. Generative feature replay for class-incremental learning. In *Proceedings of the IEEE/CVF Conference on Computer Vision and Pattern Recognition Workshops*, pages 226–227, 2020.
- [16] Simone Magistri, Tomaso Trinci, Albin Soutif-Cormerais, Joost van de Weijer, and Andrew D Bagdanov. Elastic feature consolidation for cold start exemplar-free incremental learning. *arXiv preprint arXiv:2402.03917*, 2024.
- [17] Jie Zhang, Chen Chen, Weiming Zhuang, and Lingjuan Lyu. Target: Federated class-continual learning via exemplar-free distillation. In *Proceedings of the IEEE/CVF International Conference on Computer Vision*, pages 4782–4793, 2023.
- [18] Daiqing Qi, Handong Zhao, and Sheng Li. Better generative replay for continual federated learning. *arXiv preprint arXiv:2302.13001*, 2023.

- [19] Sara Babakniya, Zalan Fabian, Chaoyang He, Mahdi Soltanolkotabi, and Salman Avestimehr. A data-free approach to mitigate catastrophic forgetting in federated class incremental learning for vision tasks. *Advances in Neural Information Processing Systems*, 36, 2024.
- [20] Geoffrey Hinton, Oriol Vinyals, and Jeff Dean. Distilling the knowledge in a neural network. *arXiv preprint arXiv:1503.02531*, 2015. URL <https://arxiv.org/abs/1503.02531>.
- [21] Zhizhong Li and Derek Hoiem. Learning without forgetting. *IEEE transactions on pattern analysis and machine intelligence*, 40(12):2935–2947, 2017.
- [22] James Kirkpatrick, Razvan Pascanu, Neil Rabinowitz, Joel Veness, Guillaume Desjardins, Andrei A Rusu, Kieran Milan, John Quan, Tiago Ramalho, Agnieszka Grabska-Barwinska, et al. Overcoming catastrophic forgetting in neural networks. 114(13):3521–3526, 2017.
- [23] Friedemann Zenke, Ben Poole, and Surya Ganguli. Continual learning through synaptic intelligence. In *ICML*, pages 3987–3995. PMLR, 2017.
- [24] Arun Mallya and Svetlana Lazebnik. Packnet: Adding multiple tasks to a single network by iterative pruning. pages 7765–7773, 2018.
- [25] Jaehong Yoon, Eunho Yang, Jeongtae Lee, and Sung Ju Hwang. Lifelong learning with dynamically expandable networks. *arXiv preprint arXiv:1708.01547*, 2017.
- [26] Arun Mallya, Dillon Davis, and Svetlana Lazebnik. Piggyback: Adapting a single network to multiple tasks by learning to mask weights. pages 67–82, 2018.
- [27] Gido M Van de Ven and Andreas S Tolias. Three scenarios for continual learning. *arXiv preprint arXiv:1904.07734*, 2019.
- [28] Yuhang Ma, Zhongle Xie, Jue Wang, Ke Chen, and Lidan Shou. Continual federated learning based on knowledge distillation. In *IJCAI*, pages 2182–2188, 2022.
- [29] Xin Yang, Hao Yu, Xin Gao, Hao Wang, Junbo Zhang, and Tianrui Li. Federated continual learning via knowledge fusion: A survey. *IEEE Transactions on Knowledge and Data Engineering*, 2024.
- [30] Hanting Chen, Yunhe Wang, Chang Xu, Zhaohui Yang, Chuanjian Liu, Boxin Shi, Chunjing Xu, Chao Xu, and Qi Tian. Data-free learning of student networks. In *Proceedings of the IEEE/CVF international conference on computer vision*, pages 3514–3522, 2019.
- [31] James Smith, Yen-Chang Hsu, Jonathan Balloch, Yilin Shen, Hongxia Jin, and Zsolt Kira. Always be dreaming: A new approach for data-free class-incremental learning. In *Proceedings of the IEEE/CVF International Conference on Computer Vision*, pages 9374–9384, 2021.
- [32] Matan Haroush, Itay Hubara, Elad Hoffer, and Daniel Soudry. The knowledge within: Methods for data-free model compression. In *Proceedings of the IEEE/CVF Conference on Computer Vision and Pattern Recognition*, pages 8494–8502, 2020.
- [33] Anastasiia Usmanova, François Portet, Philippe Lalanda, and German Vega. A distillation-based approach integrating continual learning and federated learning for pervasive services. *arXiv preprint arXiv:2109.04197*, 2021.
- [34] Xuan Liu, Xiaoguang Wang, and Stan Matwin. Improving the interpretability of deep neural networks with knowledge distillation. In *2018 IEEE International Conference on Data Mining Workshops (ICDMW)*, pages 905–912. IEEE, 2018.
- [35] Alex Krizhevsky, Geoffrey Hinton, et al. Learning multiple layers of features from tiny images. *Master’s thesis, Department of Computer Science, University of Toronto*, 2009.
- [36] Leon Yao and John Miller. Tiny imagenet classification with convolutional neural networks. *CS 231N*, 2(5):8, 2015.
- [37] Sashank Reddi, Zachary Charles, Manzil Zaheer, Zachary Garrett, Keith Rush, Jakub Konečný, Sanjiv Kumar, and H Brendan McMahan. Adaptive federated optimization. *arXiv preprint arXiv:2003.00295*, 2020.
- [38] Kaiming He, Xiangyu Zhang, Shaoqing Ren, and Jian Sun. Deep residual learning for image recognition. In *Proceedings of the IEEE conference on computer vision and pattern recognition*, pages 770–778, 2016. doi: 10.1109/CVPR.2016.90.

- [39] Léon Bottou. Online algorithms and stochastic approximations. *Online learning in neural networks*, 1998.
- [40] Jia Deng, Wei Dong, Richard Socher, Li-Jia Li, Kai Li, and Li Fei-Fei. Imagenet: A large-scale hierarchical image database. In *2009 IEEE conference on computer vision and pattern recognition*, pages 248–255. Ieee, 2009. doi: 10.1109/CVPR.2009.5206848.
- [41] Pratik Chaudhari, Anna Choromanska, Stefano Soatto, Yann LeCun, Carlo Baldassi, Christian Borgs, Jennifer Chayes, Levent Sagun, and Riccardo Zecchina. Entropy-sgd: Biasing gradient descent into wide valleys. *Journal of Statistical Mechanics: Theory and Experiment*, 2019(12):124018, 2019.
- [42] Stanisław Jastrzębski, Zachary Kenton, Devansh Arpit, Nicolas Ballas, Asja Fischer, Yoshua Bengio, and Amos Storkey. Three factors influencing minima in sgd. *arXiv preprint arXiv:1711.04623*, 2017.
- [43] Nitish Shirish Keskar, Dheevatsa Mudigere, Jorge Nocedal, Mikhail Smelyanskiy, and Ping Tak Peter Tang. On large-batch training for deep learning: Generalization gap and sharp minima. *arXiv preprint arXiv:1609.04836*, 2016.
- [44] Chuan Guo, Geoff Pleiss, Yu Sun, and Kilian Q Weinberger. On calibration of modern neural networks. In *International conference on machine learning*, pages 1321–1330. PMLR, 2017.
- [45] Meelis Kull, Miquel Perello Nieto, Markus Kängsepp, Telmo Silva Filho, Hao Song, and Peter Flach. Beyond temperature scaling: Obtaining well-calibrated multi-class probabilities with dirichlet calibration. *Advances in neural information processing systems*, 32, 2019.
- [46] Dan Hendrycks and Thomas Dietterich. Benchmarking neural network robustness to common corruptions and perturbations. *arXiv preprint arXiv:1903.12261*, 2019.
- [47] Prashant Shivaram Bhat, Bahram Zonooz, and Elahe Arani. Task agnostic representation consolidation: a self-supervised based continual learning approach. In *Conference on Lifelong Learning Agents*, pages 390–405. PMLR, 2022.
- [48] Zhenyi Wang, Li Shen, Donglin Zhan, Qiuling Suo, Yanjun Zhu, Tiehang Duan, and Mingchen Gao. Metamix: Towards corruption-robust continual learning with temporally self-adaptive data transformation. In *Proceedings of the IEEE/CVF Conference on Computer Vision and Pattern Recognition*, pages 24521–24531, 2023.
- [49] Junyoung Park, Jin Kim, Hyeongjun Kwon, Ilhoon Yoon, and Kwanghoon Sohn. Layer-wise auto-weighting for non-stationary test-time adaptation. In *Proceedings of the IEEE/CVF Winter Conference on Applications of Computer Vision*, pages 1414–1423, 2024.
- [50] Linfeng Zhang, Jiebo Song, Anni Gao, Jingwei Chen, Chenglong Bao, and Kaisheng Ma. Be your own teacher: Improve the performance of convolutional neural networks via self distillation. In *Proceedings of the IEEE/CVF international conference on computer vision*, pages 3713–3722, 2019.
- [51] Jochen Bröcker. Reliability, sufficiency, and the decomposition of proper scores. *Quarterly Journal of the Royal Meteorological Society: A journal of the atmospheric sciences, applied meteorology and physical oceanography*, 135(643):1512–1519, 2009.
- [52] Tilmann Gneiting, Fadoua Balabdaoui, and Adrian E Raftery. Probabilistic forecasts, calibration and sharpness. *Journal of the Royal Statistical Society Series B: Statistical Methodology*, 69(2):243–268, 2007.
- [53] Mahdi Pakdaman Naeini, Gregory Cooper, and Milos Hauskrecht. Obtaining well calibrated probabilities using bayesian binning. In *Proceedings of the AAAI conference on artificial intelligence*, volume 29, 2015.

A FedGTG algorithm

Recall that there are n tasks T_1, T_2, \dots, T_n . At task T_1 , the system is trained using the conventional FedAVG algorithm for aggregating the weight from the clients in R communication rounds. At the end of every task, the server trains a data generator and a feature generator without using any information from the clients. From task T_2 , these two generators are sent to the clients, which combine with modified objectives to both retain knowledge and learn new tasks well. We formalize our approach in Algorithm 1 in detail. The code is available at <https://github.com/lucaznguyen/FedGTG>.

Algorithm 1 Federated Global Twin Generator

```

1: Input:
2:  $n$  tasks with  $n$  datasets  $\{\mathcal{D}_1, \mathcal{D}_2, \dots, \mathcal{D}_n\}$ .
3:  $c$  clients with  $c$  local models  $\theta$ ,  $R$  communication rounds.
4: A global model  $\theta_G$ , a data generator  $G_D$  and a feature generator  $G_F$ .
5: Procedure:
6: for  $t = 1$  to  $T$  do
7:   for  $r = 1$  to  $R$  do ▷ Each task is learned on several communication rounds
8:     Select  $k$  clients for training.
9:     if  $r > 1$  or  $t > 1$  then
10:      The server sends the global model’s weight to selected clients.
11:      if  $t > 1$  then
12:        The server sends the two generators, the global model’s weight from the previous
13:        task and the Empirical Feature Matrix to selected clients.
14:      end if
15:      end if
16:      if  $t = 1$  then
17:        Train local models  $\theta_j^{(t,r)}$  conventionally. ▷  $1 \leq j \leq k$ 
18:      else
19:        Train local models  $\theta_j^{(t,r)}$  using Algorithm 2.
20:      end if
21:      Aggregate local model updates to the server.
22:    end for
23:    Train the data generator and the feature generator.
24:    Calculate Empirical Feature Matrix  $E^t$  using synthetic features.
25:  end for

```

Algorithm 2 Client-side: Continual Learning

```

1: Input:
2: Task  $T_t$ ,  $t \geq 2$  with the dataset  $\mathcal{D}_t$  in round  $r$  has  $B$  batches.
3: The global model  $\theta_G^{(t,r)}$ , a data generator  $G_D^{t-1}$ , a feature generator  $G_F^{t-1}$ .
4: The frozen global weight  $\theta_G^{(t-1)}$  and the Empirical Feature Matrix  $E^{t-1}$ .
5: Procedure:
6: Calculate the Current Cross-Entropy Loss  $\mathcal{L}_{CE}$  using  $\mathcal{D}_t$  and Equation 9.
7: Generate synthetic data  $\mathcal{D}_S$  and synthetic features  $\mathcal{F}_S$  having  $B$  batches each.
8: Calculate the Fine-tuning Loss  $\mathcal{L}_{FT}$  using  $\mathcal{D}_t$ ,  $\mathcal{D}_S$  and Equation 11.
9: Calculate the Synthetic Logits Distillation Loss  $\mathcal{L}_{logits}$  using  $\mathcal{F}_S$  and Equation 10.
10: Calculate the EFM Loss  $\mathcal{L}_{EFM}$  using  $\mathcal{F}_S$  and Equation 12.
11: Optimize Equation 13.

```

B Experimental Setup

In this section, we detail the settings used in our experiments, including datasets, FCIL algorithms, and experimental setups.

Datasets We perform our experiments on three widely-used benchmark datasets, including the FCIL version of CIFAR-10 [35], CIFAR-100 [35] and tiny-ImageNet [36]:

- **Sequential F-CIFAR-10.** The CIFAR-10 dataset [35] consists of 60,000 32×32 color images in 10 classes, with 6,000 images per class. There are 50,000 training images and 10,000 test images. We split the training set into five disjoint subsets corresponding to 5 tasks.
- **Sequential F-CIFAR-100.** Sequential F-CIFAR-100 is constructed by dividing the original CIFAR-100 dataset [35], which contains 50,000 images belonging to 100 classes, into ten disjoint subsets corresponding to 10 tasks. In this way, each task has 5,000 images from 10 distinct categories, and each class has 500 images.
- **Sequential F-tiny-ImageNet.** Tiny-ImageNet [36] is a subset of ImageNet, containing 100,000 images of 200 real objects. We follow settings in [19] to form the Sequential F-tiny-ImageNet. In particular, we split the original dataset into ten non-overlapping subsets. We consider each subset as a task whose images are labeled by 20 different classes, and each class has 500 samples.

FCIL Baselines In addition to our FedGTG, we also include one regularization-based method, **FLwF-2T** [33], and two generative-based methods, **TARGET** [17] and **MFCL** [19]. **FLwF-2T** utilize knowledge distillation both on the server side and client side to ease the catastrophic forgetting issue. **TARGET** utilizes a global model to transfer knowledge from past tasks to the current task while also training a generator to generate synthetic data, mimicking the overall data distribution across clients. **MFCL** employs a generative model to create samples from previous distributions, which are then combined with training data to prevent catastrophic forgetting. Both of these algorithms ensure privacy by training the generative model on the server using data-free techniques after each task without client data retrieval.

Implementation Details Table 2 shows our settings and the hyper-parameter tuning for each dataset.

C Generative model setup

Data Generative Model Architecture Figure 7 presents the architecture of the data generative models used for the Sequential F-CIFAR-10, Sequential F-CIFAR-100, and Sequential F-tiny-ImageNet dataset. In all experiments, the global model is based on the ResNet-18 backbone.

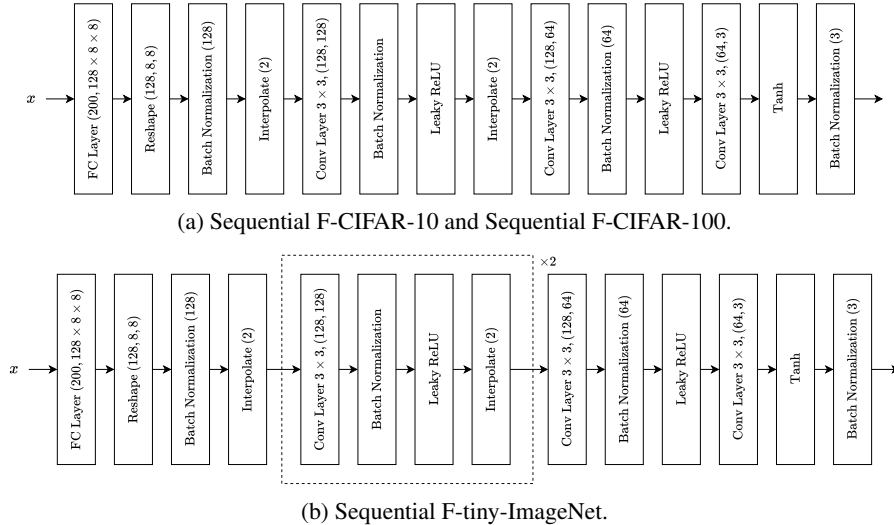


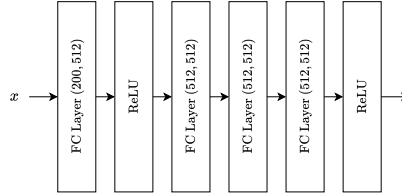
Figure 7: Architecture of the data generative model across three datasets.

Feature Generative Model Architecture The architecture of the feature generative models is illustrated in Figure 8, which employed for the Sequential F-CIFAR-10, Sequential F-CIFAR-100,

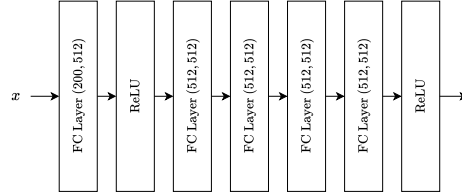
Setting	Dataset	CIFAR-10	CIFAR-100	tiny-ImageNet
Experimental setup	Image size	32×32	32×32	64×64
	Task number	5	10	10
	Classes per task	2	10	20
	Samples per task	5000	500	500
	Learning rate	0.1	0.1	0.1
	Weight decay	0.1	0.1	0.1
	Batch size	32	32	32
	Synthetic batch size	32	32	128
	Communication round	100	100	100
Hyper-parameter tuning	Local epoch	10	10	10
	λ_{IE}	1.0	1.0	1.0
	λ_{batch}	1.0	1.0	1.0
	λ_{smooth}	1.0	1.0	1.0
	λ_{FIE}	1.0	1.0	1.0
	$\lambda_{current}$	1.5	1.5	2.0
	λ_{FT}	1.0	1.0	1.0
	λ_{logits}	0.1	0.1	0.05
	λ_{EFM}	0.005	0.005	0.005
	λ_E	10.0	10.0	10.0
η	0.1	0.1	0.1	

Table 2: Detail settings across three datasets.

and Sequential F-tiny-ImageNet datasets. As the outputs are feature vectors, only fully connected layers are needed.



(a) Sequential F-CIFAR-10 and Sequential F-CIFAR-100.



(b) Sequential F-tiny-ImageNet.

Figure 8: Architecture of the data generative model across three datasets.

Information generation To create synthetic data, clients sample i.i.d. noise, which is used to determine the classes through the application of the argmax function to the first q elements, where q represents the total number of classes observed. Since the noise is sampled i.i.d., each class has an equal probability of $\frac{1}{q}$ for sample generation.

D Additional results

In this section, we show additional results about the robustness of testing on natural images across our method and other FCIL methods. Figure 5 shows the last 09 augmentations of the CIFAR-100 dataset averaged over three different runs. Our approach still outperforms MFCL and TARGET in terms of test accuracy.

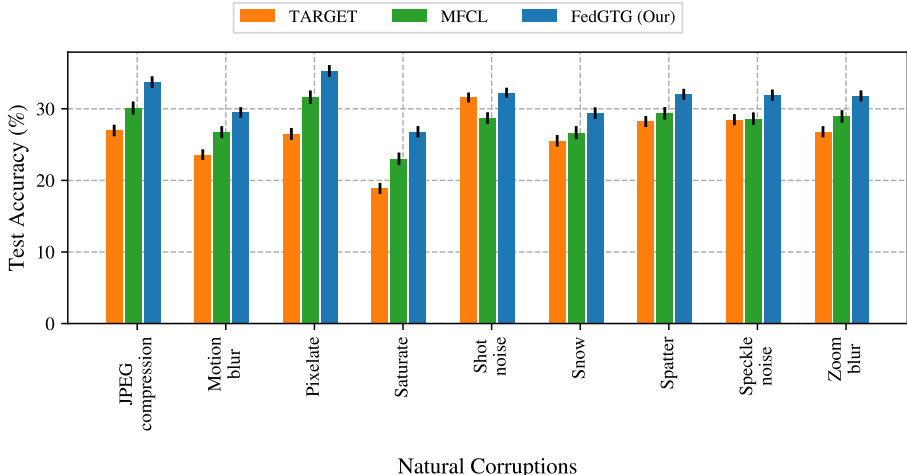


Figure 9: Robustness to natural corruptions.

E Ablation Study

w/o Loss	\mathcal{A}^1	\mathcal{A}^2	\mathcal{A}^3	\mathcal{A}^4	\mathcal{A}^5	\mathcal{A}^6	\mathcal{A}^7	\mathcal{A}^8	\mathcal{A}^9	\mathcal{A}^{10}	\mathcal{A}	\mathcal{F}
\mathcal{L}_{IE}	72.40	56.60	46.96	38.22	33.18	30.73	28.50	25.05	23.98	22.37	33.95	37.31
\mathcal{L}_{batch}	72.40	55.62	48.67	41.25	33.48	30.08	27.10	22.98	22.48	21.41	33.67	41.42
\mathcal{L}_{smooth}	72.40	57.15	49.10	41.85	39.44	37.58	34.67	31.15	30.50	29.20	38.96	29.36
\mathcal{L}_{FIE}	72.40	56.35	47.96	37.22	34.18	32.61	29.82	26.17	24.98	23.03	34.70	33.42
\mathcal{L}_{FT}	72.40	41.80	34.67	29.25	22.68	17.60	15.17	13.06	12.59	12.09	22.10	11.66
\mathcal{L}_{logits}	72.40	57.15	49.77	43.05	39.36	37.72	35.67	33.19	32.73	31.62	40.03	25.35
\mathcal{L}_{EFM}	72.40	56.30	48.77	42.53	39.56	37.28	35.37	31.91	31.66	29.92	39.26	27.38
FedGTG (ours)	72.40	57.95	54.85	50.20	47.45	44.95	41.00	39.01	37.92	36.46	46.42	18.66

Table 3: Ablation study for FedGTG on Sequential F-CIFAR-100.

In this section, we highlight the significance of each loss within our proposed framework, analyzing both server and client contributions by sequentially removing components to observe their effects. Table 3 shows our results, where each row corresponds to the removal of a specific loss component, and the columns display the corresponding Average Accuracy (\mathcal{A}^t), for $1 \leq t \leq 10$, Average Incremental Accuracy (\mathcal{A}), and Average Forgetting (\mathcal{F}) from our proposed method. Specifically, we can see that the performance of the model is influenced by generative models, as poorly trained ones result in low AIA and high AF compared to others. Nevertheless, the Fine-tuning Loss has the lowest AF among all just because it did not learn tasks well (lowest AIA). The final two rows illustrate how the feature-constraining losses (\mathcal{L}_{logits} and \mathcal{L}_{EFM}) impact the performance of the global model, where the decrease in accuracy demonstrates the importance of these two losses.